

---

# Investigation of main-chamber and divertor recycling in DIII-D using tangentially viewing CID cameras

---

M. Groth,<sup>a</sup> T.W. Petrie,<sup>b</sup> G.D. Porter,<sup>a</sup> M.E. Fenstermacher,<sup>a</sup>  
N.H. Brooks<sup>b</sup>

<sup>a</sup> Lawrence Livermore National Laboratory, Livermore, CA 94550, USA

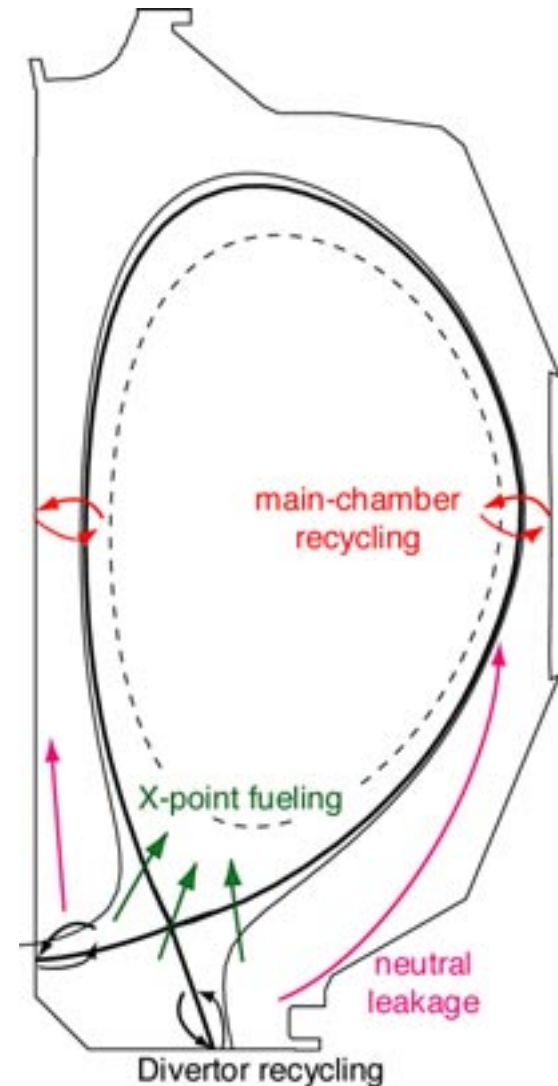
<sup>b</sup> General Atomics, San Diego, CA 92186, USA

Presented at the 30th EPS Conference on Controlled Fusion and Plasma  
Physics, July 7-11, 2003, St Petersburg, Russia



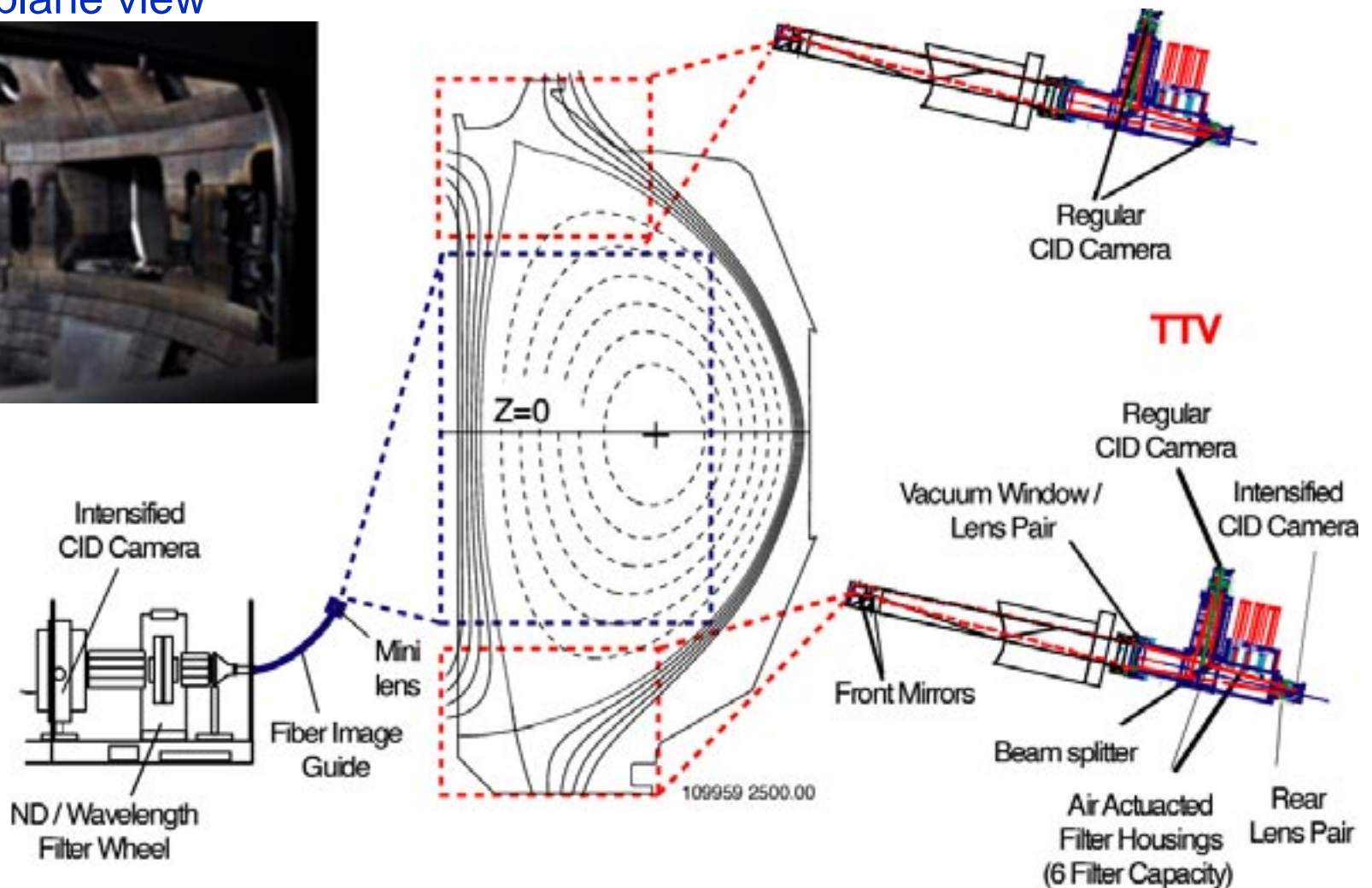
# Objective: How significant is main-chamber recycling to core plasma fueling and impurity content?

- Undesired impurity source “main chamber”
- Alcator C-Mod [1] and experiments in DIII-D reported significant contribution of main-chamber recycling (MCR) to core plasma fueling and impurity content
  - » Under which plasma conditions is main-chamber recycling significant?
  - » Toroidal and poloidal distribution of wall fluxes?
- Spatially limited diagnostic coverage of main-chamber wall in DIII-D, view **outer wall SOL** at / around tokamak midplane
- Introduction of tangentially viewing midplane camera to better benchmark numerical models
- ⇒ Use codes to evaluate significance of MCR

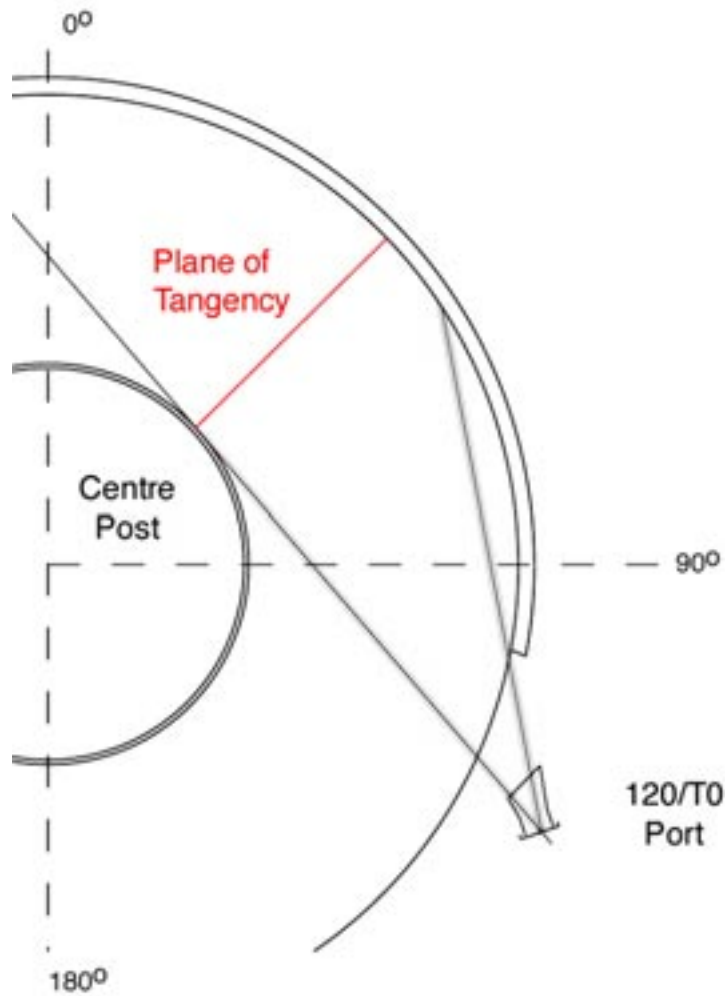


# Assess recycling using tangentially viewing CID cameras (upper and lower divertor + inner SOL)

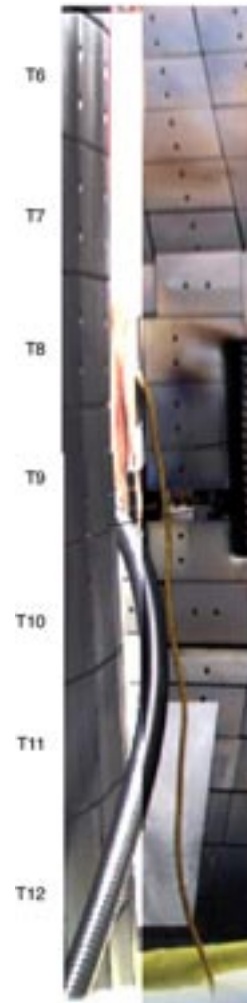
Midplane view



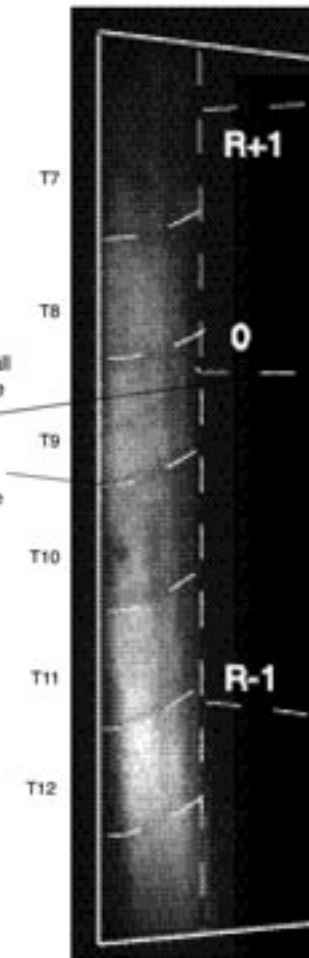
# Viewing geometry I: Tangent at inner wall ~ 45° toroidally, 0.75m above and below midplane



Standard camera



CID

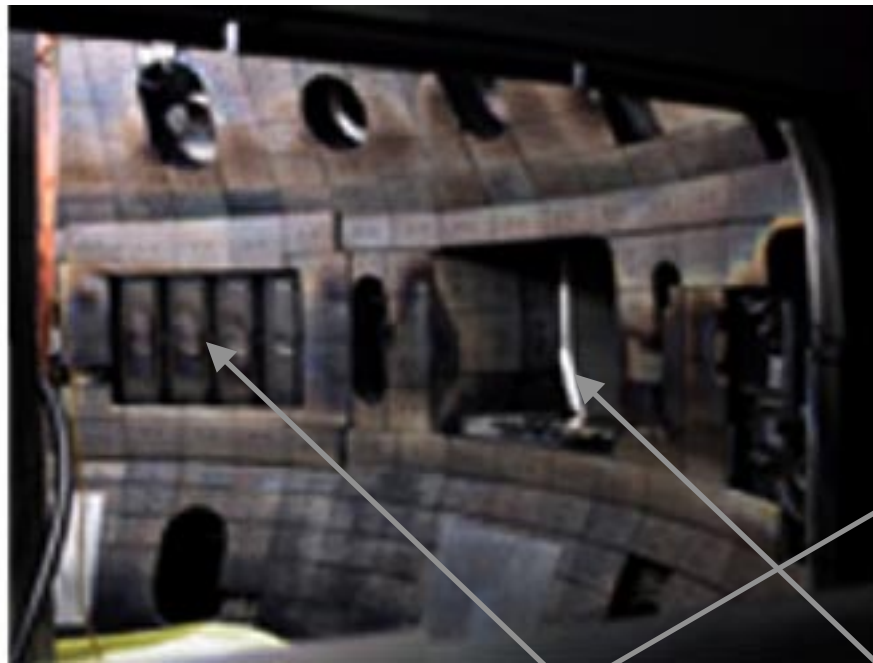


1.5m

# Viewing geometry II: Outer wall coverage ~ 60°, ~ R-1 → R+1 ports at plane of tangency

---

Standard camera



0° ICRF  
Antenna

30°  
NBI duct

CID camera through image guide

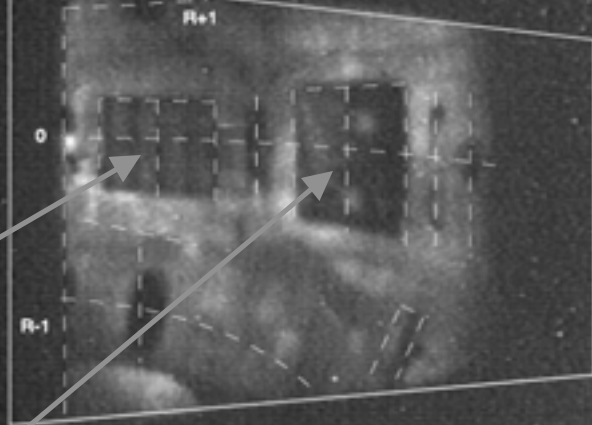
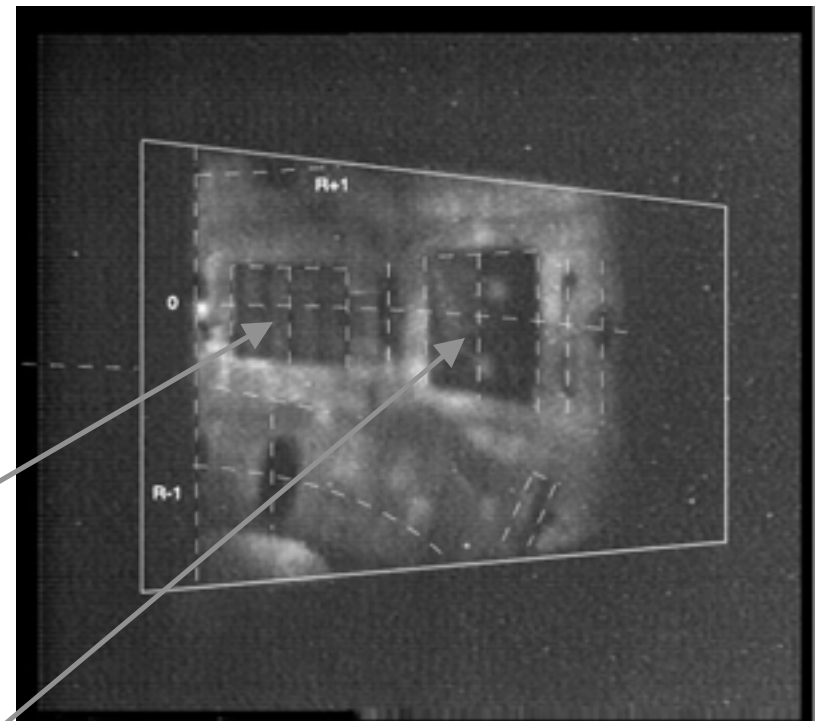
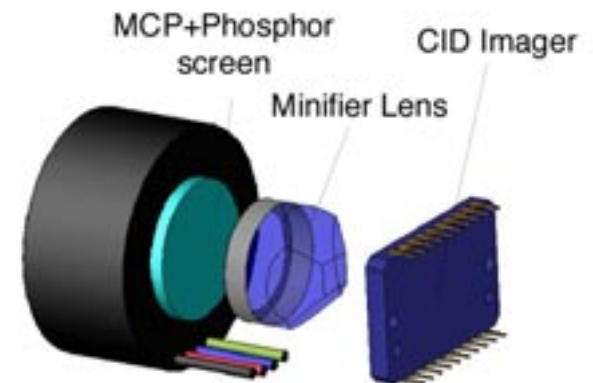


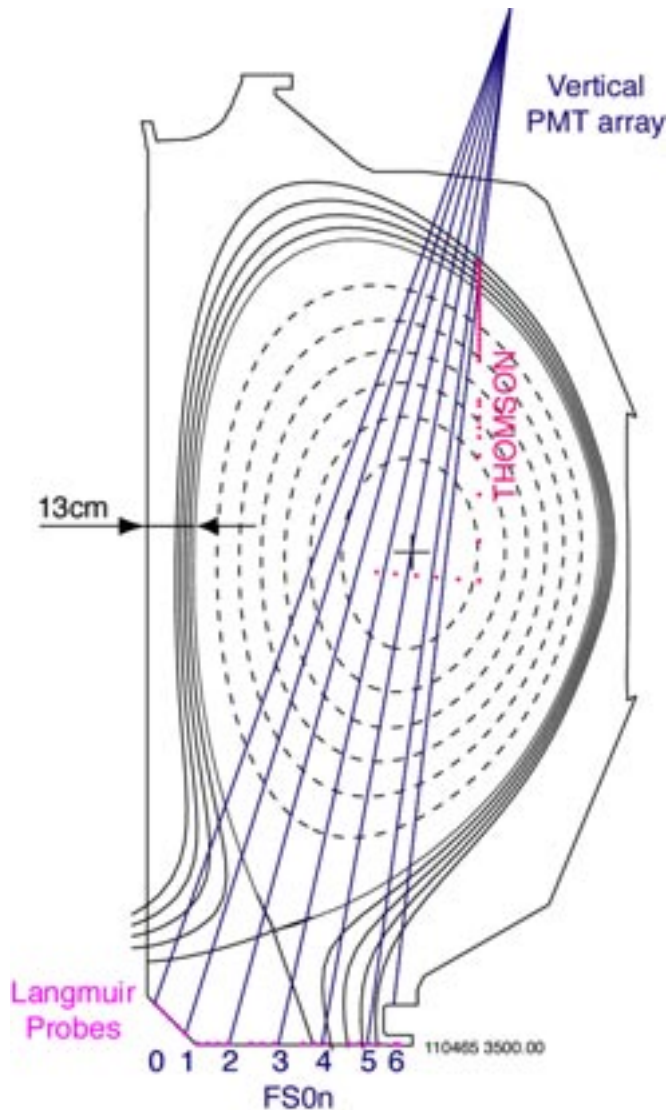
# Image data from CID cameras, poloidal emission profiles using tomographic reconstruction [2,3]

---

- Imager = radiation hardened charge-injected device (CID) camera, 8bit dynamic range
- DEP GEN II intensifier
  - » Adjustable gain, max.  $\sim 10000$ , gating down to microseconds
- Measurement of line emission profiles using interference filters
- Midplane camera latest addition to TTV system (2002):
  - » Intensified CID camera
  - » SCHOTT glass fiber image guide (**400x400 pixel elements**) connecting port optics with filter/ camera assembly
  - » Field-of-view: **1m x 1.5m of the inner SOL**, outer SOL 1m x 0.8m optional
  - » Reconstruction of 2D profiles using Abel inversion and tomographic reconstruction technique

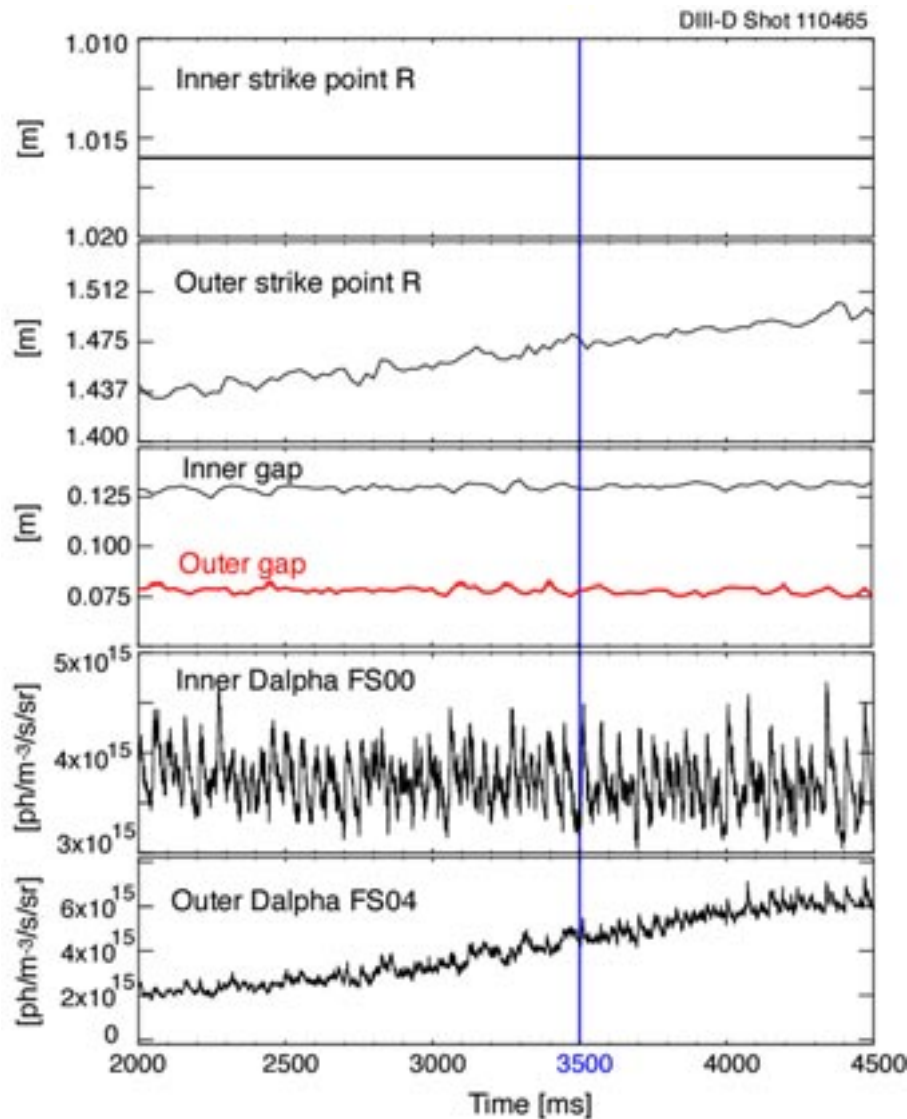


# Main-chamber recycling (MCR) in low-density L-mode plasmas (SAPP)



- Simple-As-Possible-Plasmas (SAPP) [4] = quiescent L-mode plasmas, i.e no ELMs
- Lower single null configuration; optimized for diagnosis of **outer** divertor leg
  - » Inner strike point on the center post
  - » Sweep outer strike point for profile data
  - » Inner gap 13cm
- Repeat of identical discharges for diagnostic purposes
- Low core density:  $n/n_{GW} \sim 0.2$ , low beam heating power  $\sim 0.5\text{MW}$ , quiescent - no core MHD mode
- Well-attached outer leg divertor plasma,  $T_{e, \text{plate}} \sim 25\text{-}30\text{eV}$

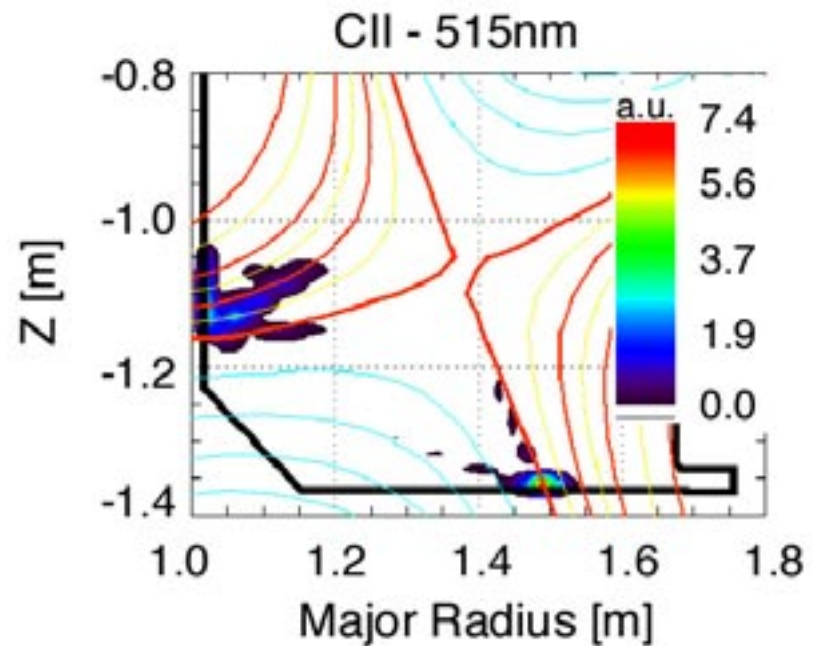
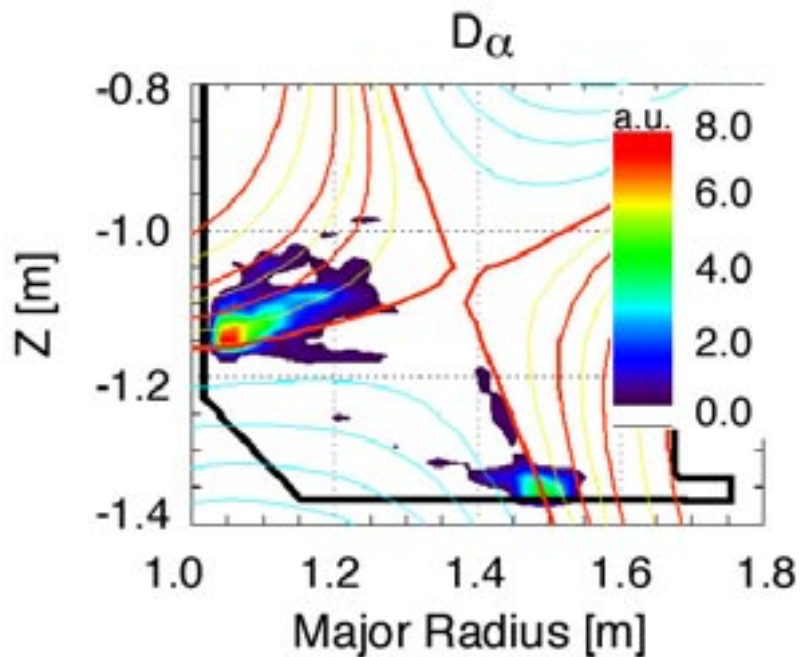
# Slow sweep of outer strike point for divertor density and temperature measurement



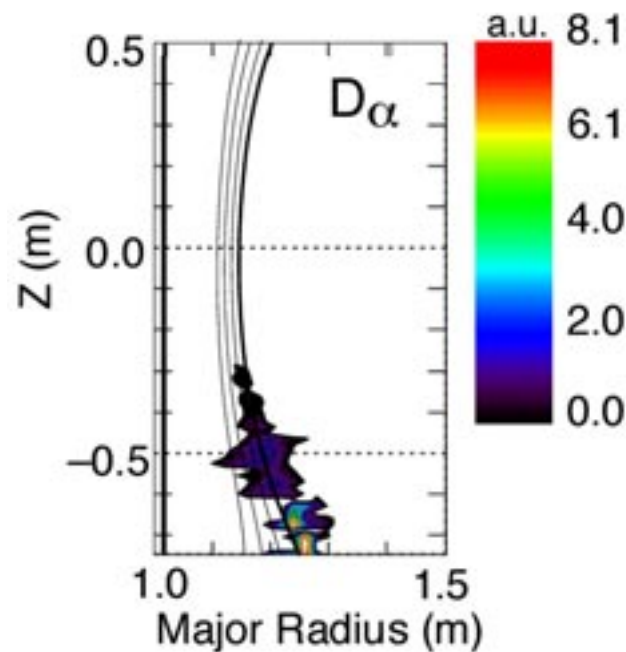
- Slow sweep of outer strike point to scan divertor plasma over Divertor Thompson scattering view cords → 2D  $n_{e,div}$  and  $T_{e,div}$
  - LPs: density and temperature profiles at target plates
  - Inner strike point fixed, but inner gap slightly increasing
  - As plasma swept over PMT array line-of-sights, outer  $D_\alpha$  (and CIII) increase; inner fixed
- Combination of data over sweep to obtain emission profile with better radial resolution

# Asymmetric $D_\alpha$ and CII divertor emission profiles, partially detached inner divertor plasma

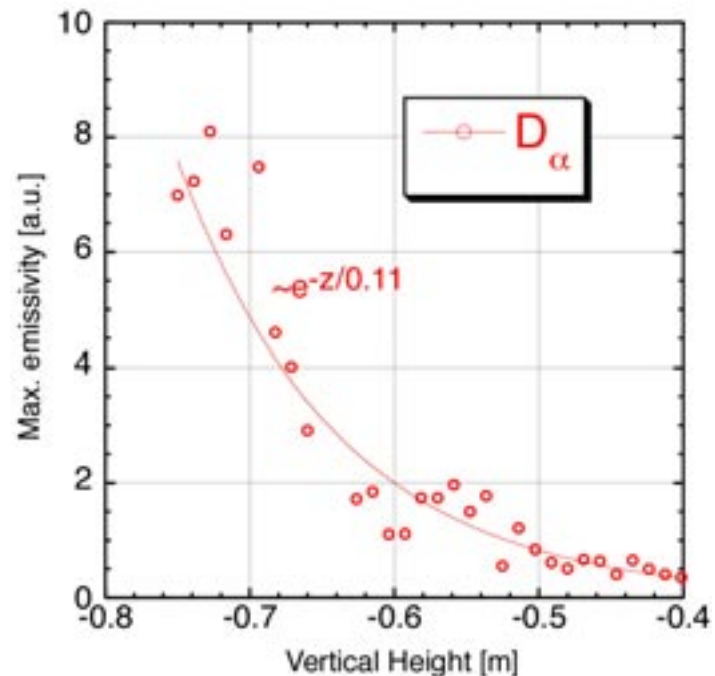
- Extended  $D_\alpha$  emission profile along inner divertor leg, emission twice as high at inner strike zone as compared to outer strike zone
- CII emission highly localized at inner and outer strike zones, ~three times higher at the outer than at the inner strike zone



# Max. $D_\alpha$ emission inside core plasma near x-point $\rightarrow$ divertor is powerful fueling source



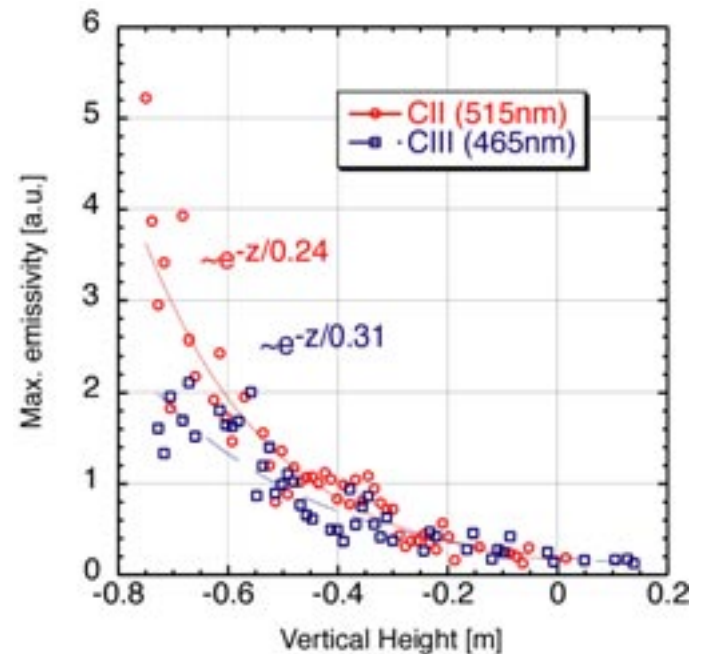
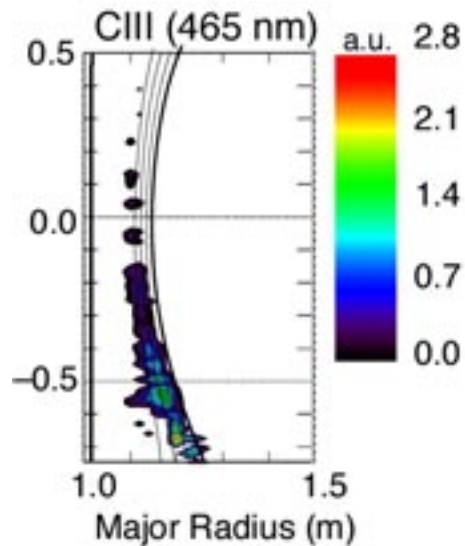
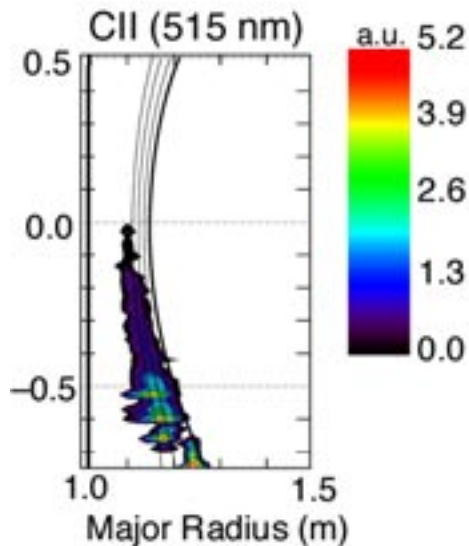
Poloidal decay of  $D_\alpha$  emission



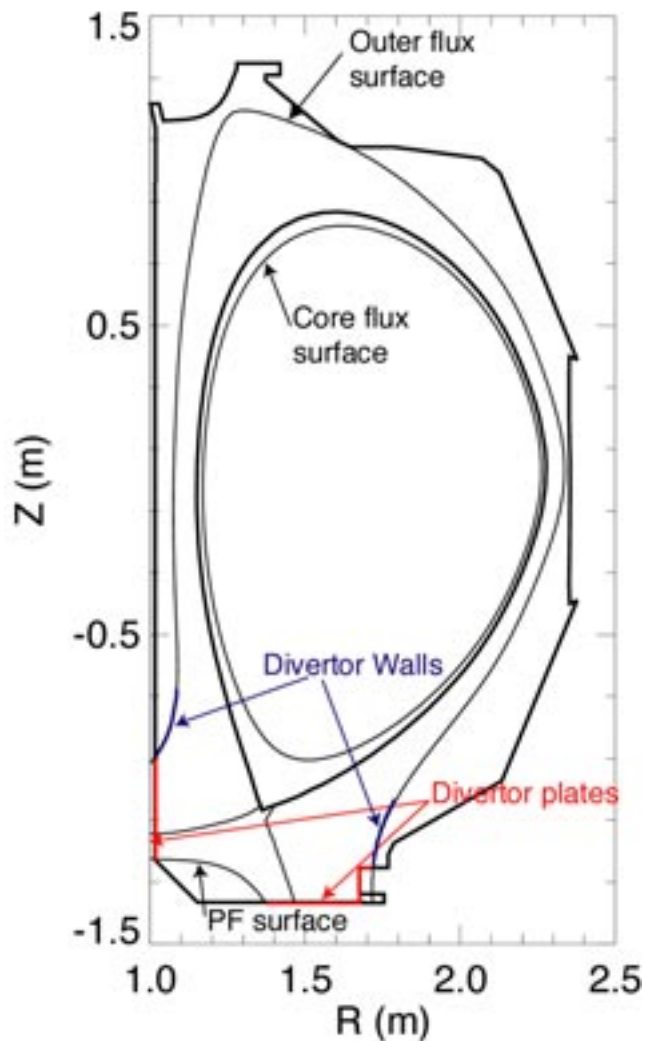
- Tomographic reconstruction performed for entire image, negligible emission from outer wall
- $D_\alpha$  emission dominant in region adjacent to lower x-point, decays poloidally toward midplane: tenfold within 0.5m poloidally

# Poloidally asymmetric CII and CIII midplane profiles, strongly weighted toward lower divertor

- CII and CIII emission found in SOL only ( $T_e < 10\text{eV}$ ), CIII emission more poloidally extended, closer to separatrix
- Ratio of peak divertor to midplane emission:  $10^3 - 10^4$
- Various routes for carbon to enter camera view conceivable, higher degree of poloidal symmetry expected if main walls were the primary source



# UEDGE modeling: SOL, diffusive radial transport, carbon from divertor plates and walls

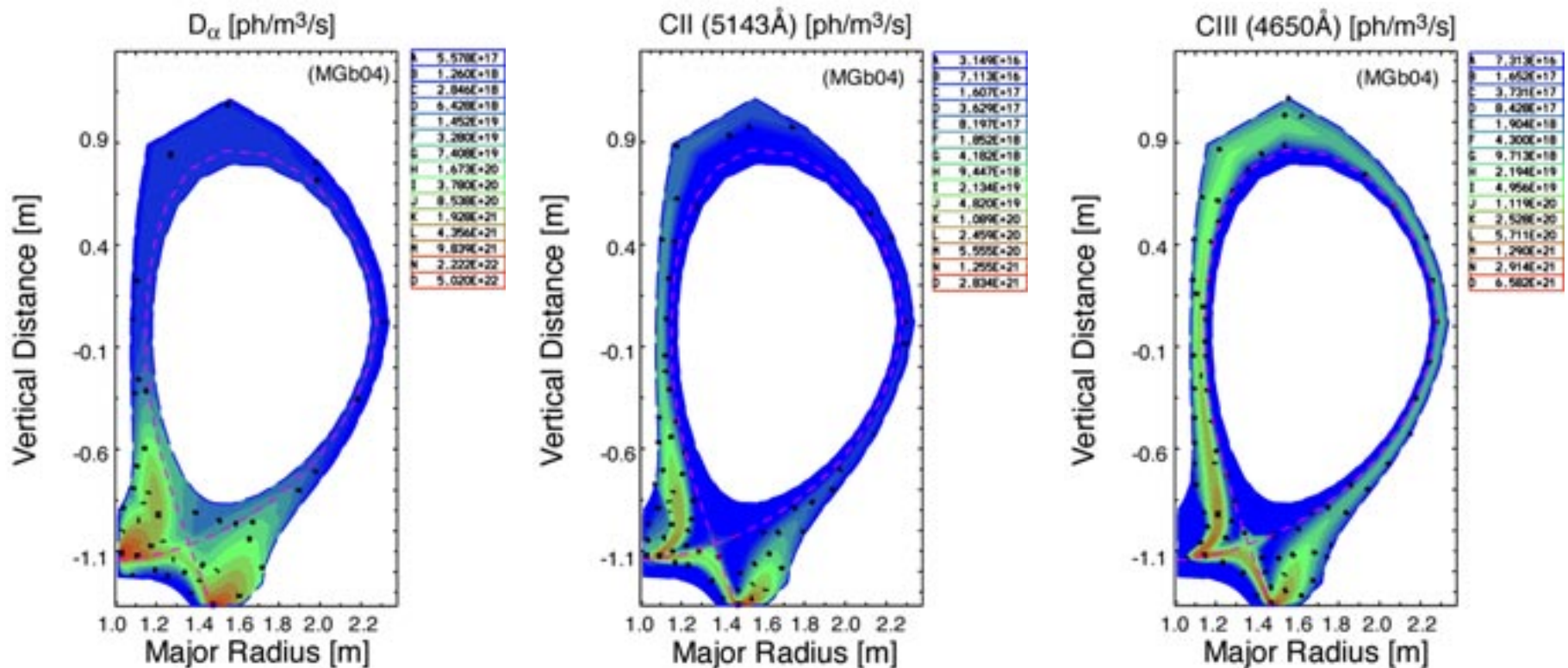


- UEDGE [5]: Classical parallel transport, w/drifts
- Diffusive radial transport, spatially constant diffusivities, obtained by matching exp. SOL  $n_e$  and  $T_e$  profiles:
  - »  $D_{\perp} = 0.2\text{m}^2/\text{s}$ ,  $\chi_e = \chi_i = 0.8\text{m}^2/\text{s}$
- Carbon origin:
  - » Physical and chemical sputtering at plates using published data [6,7]
  - » Chemical sputtering at outer boundary
  - » No recycling of carbon
- Carbon transport:
  - » Force balance model for carbon impurities in parallel B-field direction [8]:

$$F_Z = -\frac{1}{n_Z} \frac{dp_Z}{ds} + m_Z \frac{(v_i - v_Z)}{\tau_S} + ZeE + \alpha_e \frac{d(kT_e)}{ds} + \beta_i \frac{d(kT_i)}{ds}$$

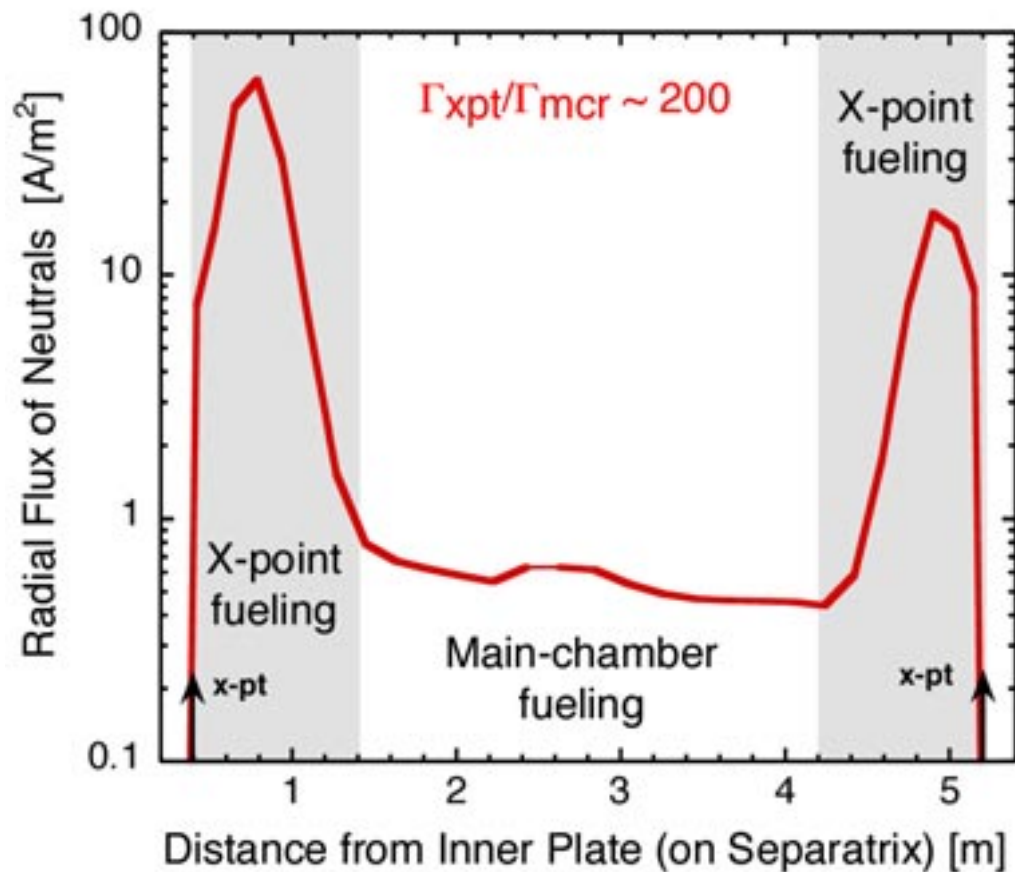
# UEDGE captures most of emission profile features → significant $D_\alpha$ emiss. around x-point

- CII / CIII emission outside separatrix only, CIII emission well off inner plate → **partially detached inner divertor plasma**
- CIII more poloidally symmetric than CII → **consistent with experimental data**
- Reduced emission in view of midplane camera by  $10^3$  to  $10^4$  (**consistent w/exp.**)



# Dominant fueling source from x-point region calculated by UEDGE

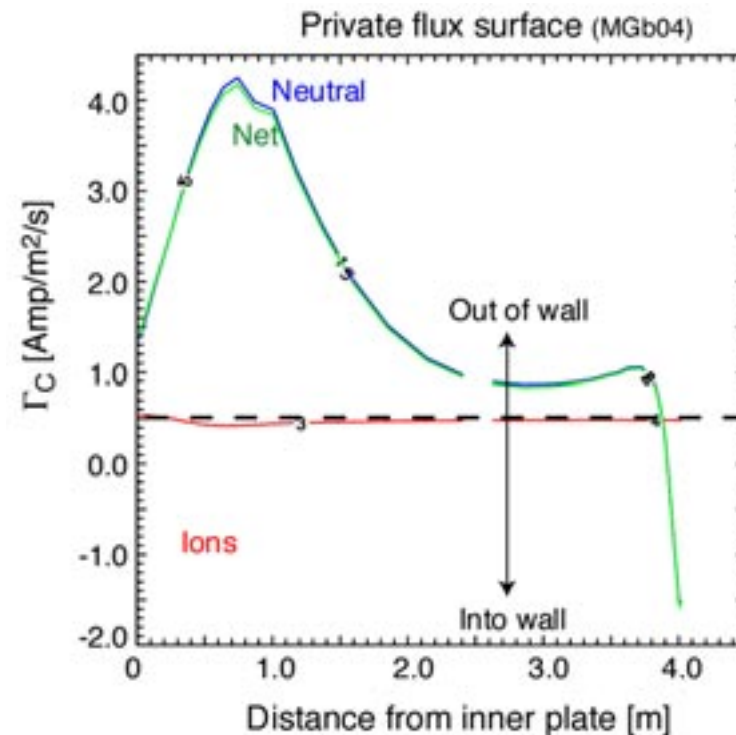
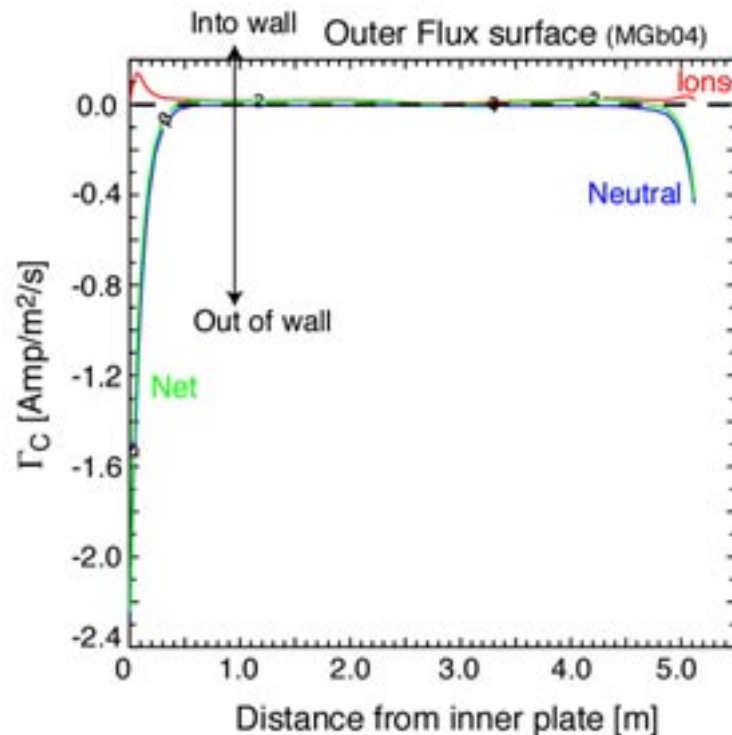
## Poloidal $D^0$ flux into core plasma



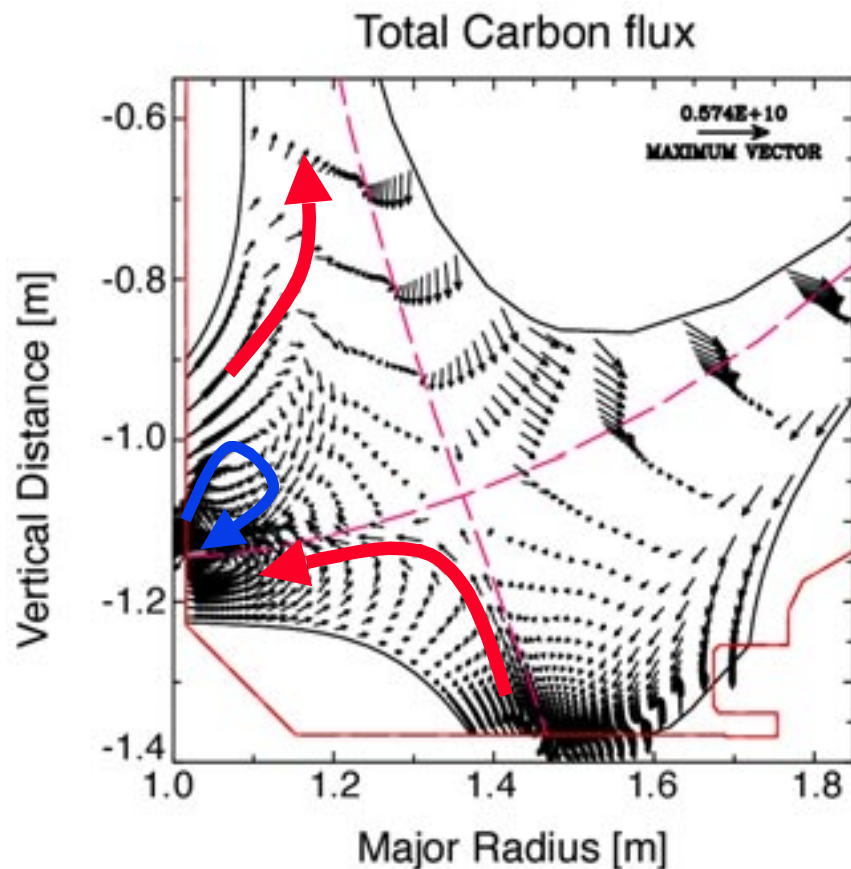
- Integrate  $D^0$  fluxes into core around x-point (shaded area) and main-chamber region
  - Ratio of  $D^0$  influxes from x-point region to main chamber  $\sim 200$
- ⇒ Low-density L-mode plasma very likely to be dominated by x-point fueling

# Transfer of chemically sputtered carbon from divertor walls to target plates

- P-C sputtered material from target plates mostly redeposited onto plates
- Neutral carbon away from plates arises from chemical sputtering at divertor walls (where  $n_0$  is high)
- Divertor wall source localized within 50 cm away from plate

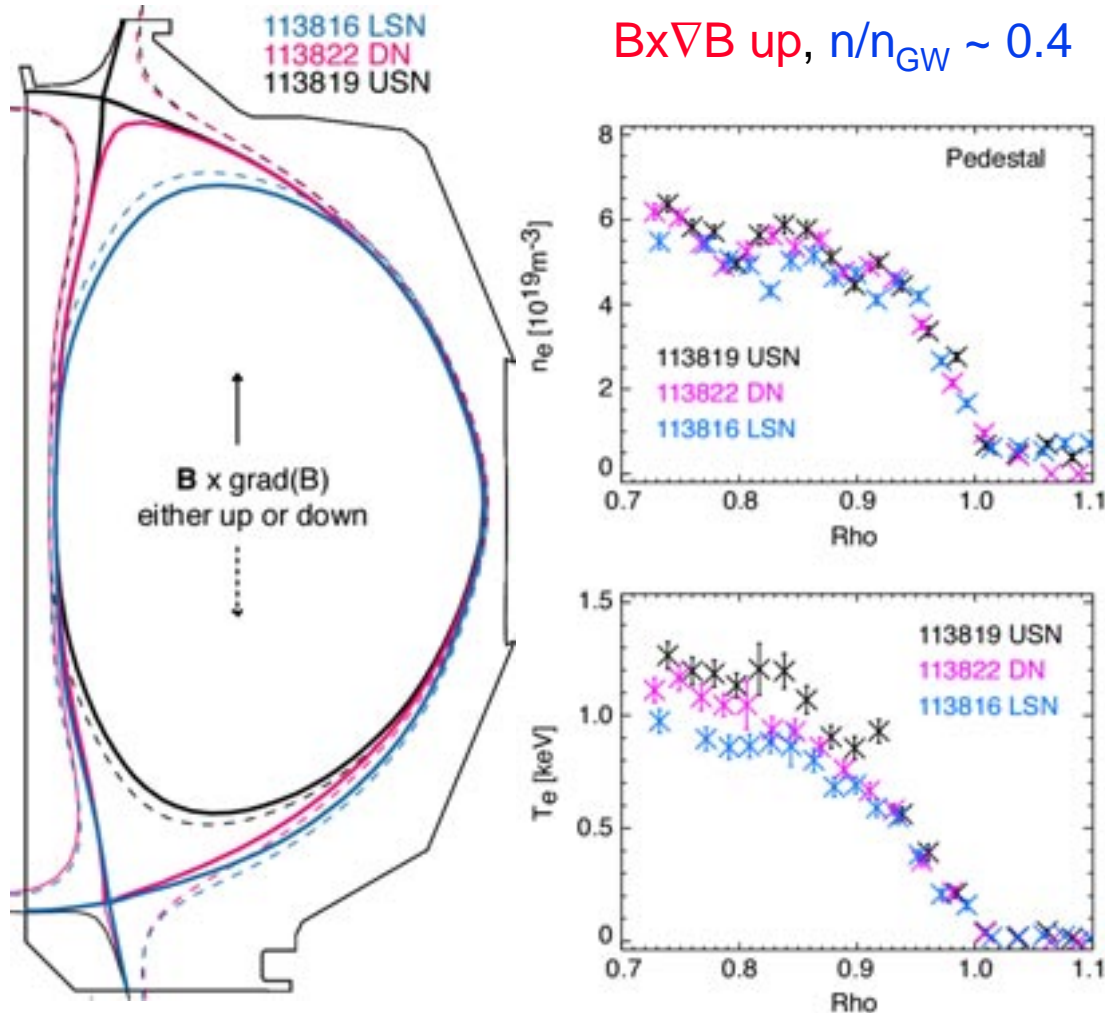


# Main SOL (and core) carbon combination of sputtering and complex ion transport



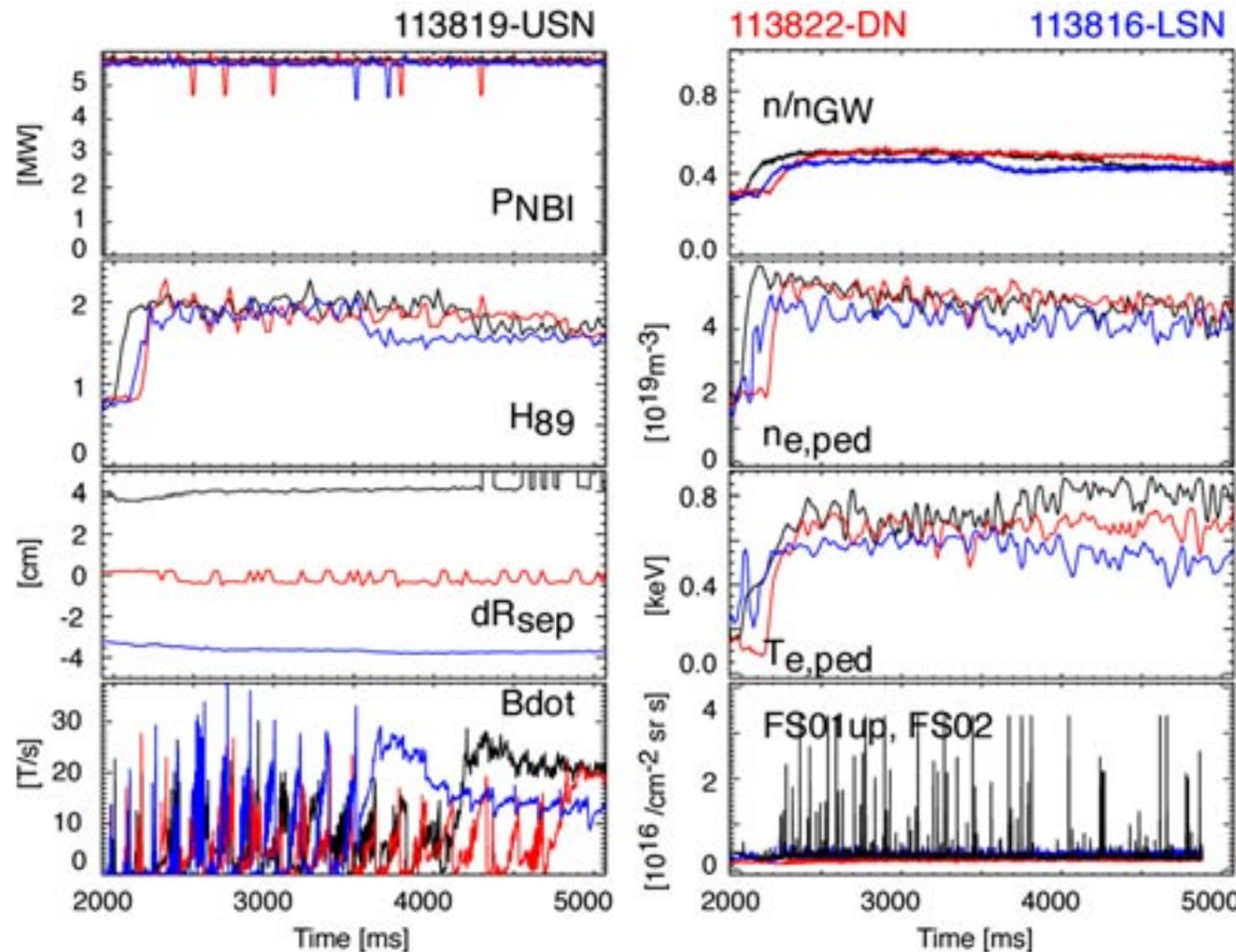
- Carbon from PF swept to inner plate by  $\mathbf{E} \times \mathbf{B}$  associated with large  $E_r$  near separatrix
- Circulation of carbon around strike zones: sputtering and redeposition
- Chemical sputtering at divertor walls up to 0.5m above the plate
- ⇒ (Net)transfer of carbon from divertor walls to target plates
- Above  $Z > -0.8\text{m}$ , ion temp. gradient force exceeds friction with background ions
- ⇒ Carbon ions transported upstream along inner main SOL

# MCR in low and medium density ELMy H-mode in balanced and unbalanced double-null config.



- ELMy H-mode:
    - »  $H_{89} \sim [1.8, 2.2]$
    - »  $I_p = 1.3 \text{MA}$ ,  $B_T = 2.0 \text{T}$
    - »  $P_{\text{NBI}} = 5.5 \text{MW}$
  - Vary magnetic balance for effect of divertor geometry ( $dR_{\text{sep}} = 0, \pm 4 \text{cm}$ )
  - Vary  $B_T$  direction for effect of  $\mathbf{B} \times \nabla \mathbf{B}$  and  $\mathbf{E} \times \mathbf{B}$  drifts
  - $n/n_{GW} \sim [0.4, 0.6]$ , well-matched  $n_{e,\text{ped}}$
- ⇒  $T_{e,\text{ped}}$  varies significantly with configuration (up to 40%)

# Similar $n_{e,ped}$ , but variations in $T_{e,ped}$ for otherwise similar plasmas in USN, DN and LSN

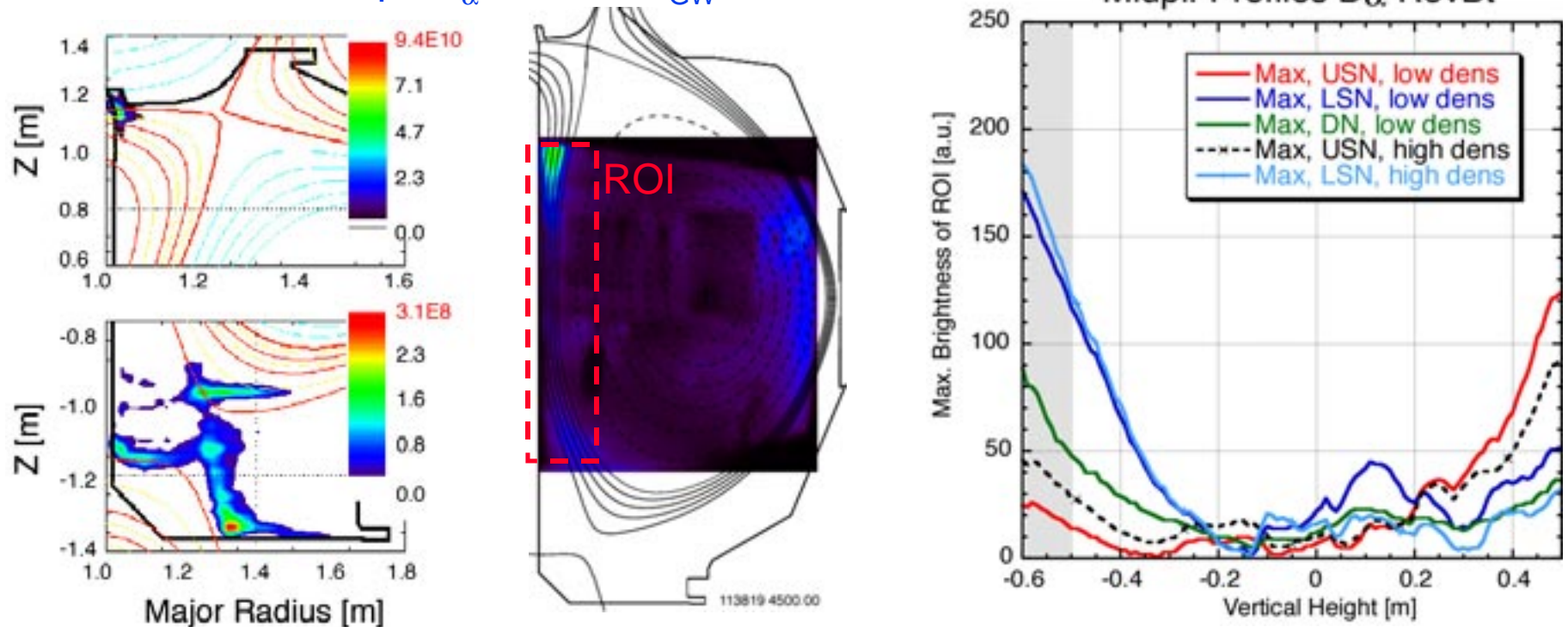


- $H_{89} \sim 1.8-2.2$
- Reduced  $\langle n_e \rangle$  due to core MHD
- $n/n_{GW} \sim 0.42$
- $T_{e,ped} [USN] > T_{e,ped} [DN] > T_{e,ped} [LSN]$
- ELM amplitude larger in the upper divertor in USN than in lower divertor in LSN

# Poloidally asymmetric $D_\alpha$ emission profile, weighted toward primary divertor(s)

- In USN:  $D_\alpha$  peaks at inner strike zone in upper div. (consistent with **ExB drift**), in lower divertor maps “extended” div. legs
- **Difference in emission between the two divertors: ~ two orders of magnitude**
- In LSN and DN,  $D_\alpha$  dominant at outer strike points in upper and lower divertor

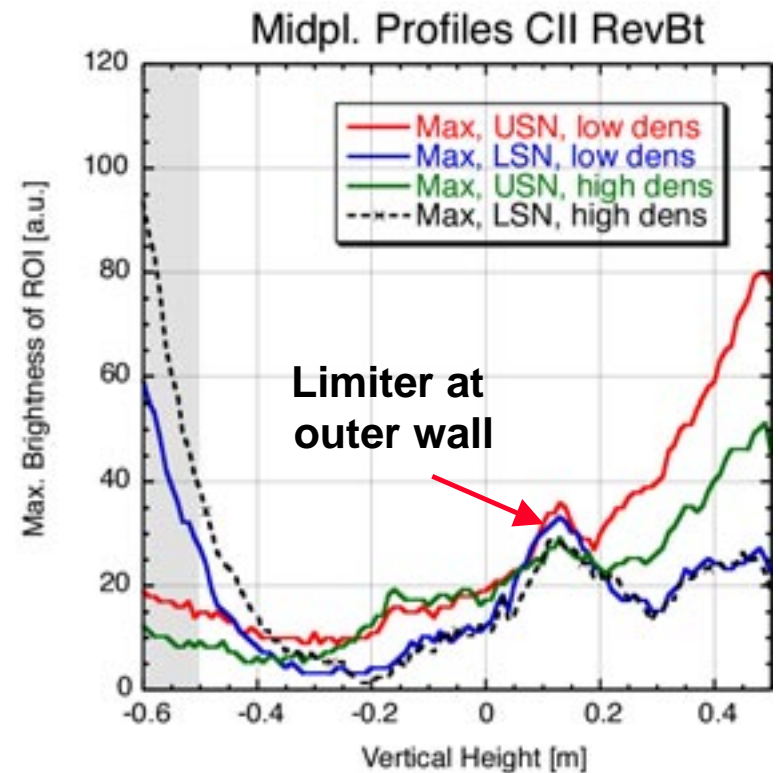
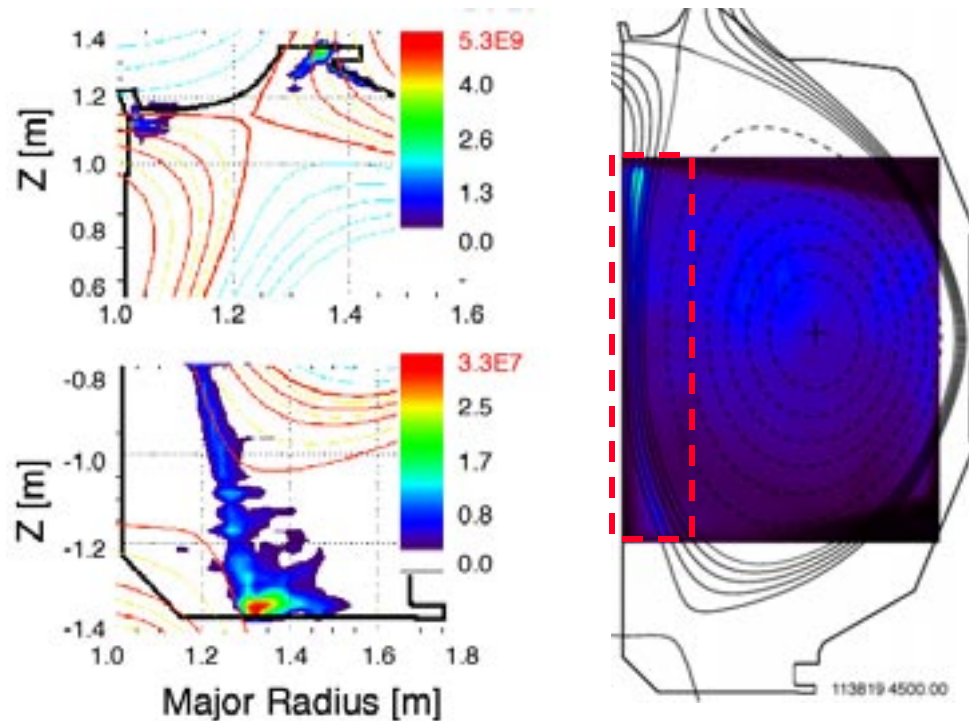
Div. and Midpl.  $D_\alpha$ , USN,  $n/n_{GW} \sim 0.4$



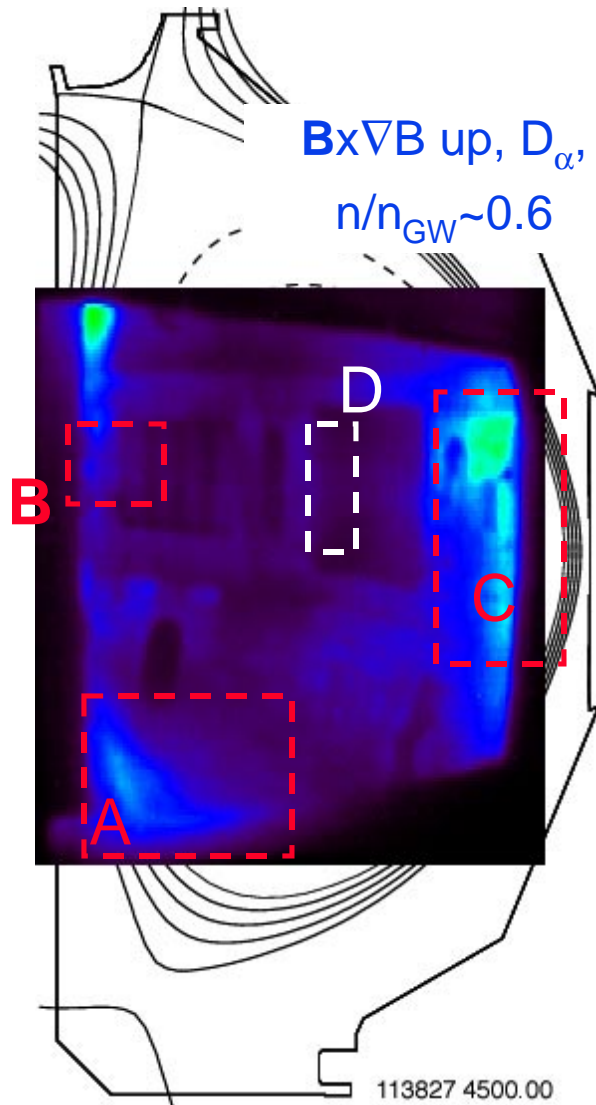
# CII and CIII profiles also weighted toward divertor(s), CIII more extended

- CII emission peaks at **outer** strike zones in USN, DN, LSN, in lower divertor  
CII maps “extended” div. legs
- CIII emission in LSN indicated **partially detached lower divertor**, while in USN plasma remained **attached to upper target plates**

Div. and Midpl. CII (515nm), USN,  $n/n_{GW} \sim 0.4$



# Assessment of **outer wall reflection** using numerical and experimental tools in progress



- With increasing  $P_{\text{NBI}}$  and density, **reflection and/or local recycling outer wall** complicate analysis
- Areas affecting all three wavelengths
  - » ADP baffle (A) - adjacent to lower x-point region
  - » ICRF antenna guard limiter (B) - above midplane
  - » Outer wall region, where view becomes more tangent with outer SOL (C)
  - » Intensity of reflection varies with power, density and magnetic configuration
- Area also affecting CII/CIII profiles,
  - » Neutral beam duct guard limiter (D)

# Summary and Conclusions

---

- New spectroscopic analysis of SOL assessed main-chamber recycling in L-mode at  $n/n_{GW} \sim 0.2$ , and in ELMy H-mode at  $n/n_{GW} \sim 0.4$  and  $0.6$

- Experimental results:
  - » Poloidally **asymmetric**  $D_\alpha$ , CII, and CIII emission profiles in the inner SOL, weighted toward primary divertor(s)
  - »  **$D_\alpha$  emission inside LCFS** at x-point region indicates strong x-point source
- Modeling results using UEDGE consistent with experimental data
- ⇒ X-point fueling contributes **two orders of magnitudes more** to core plasma fueling than main walls!

- Carbon modeling with purely diffusive radial transport in UEDGE
  - » Chemically sputtered carbon from the divertor walls and private flux region is transferred to the target plates
  - » A fraction of carbon from divertor region reaches upstream SOL (and hence core) at high field side due to dominant  $\nabla T_i$  force in region above x-point; consistent with experiment

# References

---

- [1] LaBombard, B., *et al.*, Nucl. Fusion **40**, 2041 (2000)
- [2] Fenstermacher, M.E., *et.al.*, Phys. Plasma **4**, 1761 (1997)
- [3] Groth, M., *et al.*, Rev. Sci. Instrum. **74**, 2064 (2003)
- [4] Stangeby, P.C., *et al.*, J. Nucl. Mater. **313-316**, 883 (2003)
- [5] Rognlien, T.D., *et al.*, J. Nucl. Mater. **196-198**, 347 (1992)
- [6] Davis, J.W., and Haasz, A.A., J. Nucl. Mater. **241-243**, 347 (1997)
- [7] Eckstein, W., *et al.*, J. Nucl. Mater. **248**, 1 (1997)
- [8] Neuhauser, J., *et al.*, Nucl. Fusion **24**, 39 (1984)